$$t = -\frac{r\rho}{3\bar{\varepsilon}\sigma}\int_{T_1}^{T_2}\frac{C_P(T)\,dT}{(T^4 - T_e^4)} \qquad (4)$$

Thus, cooling time is seen to be proportional to particle radius and inversely proportional at mean emissivity. For $\bar{\varepsilon} = 0.25$ and particle radii 5 μm, cooling times are ~ 2 sec for 10-μm radiation. With particle exhaust velocities of 1500 to 2500 m/sec, the radiating plume will be 6 to 10 km long, with the brightest parts within 0.6 to 1.0 km of the rocket nozzle. Particles do not spend much time at the higher temperatures, but cool relatively quickly to lower temperatures. Thus, the total cooling time is very insensitive to particle initial temperature. The most important factors in cooling time are mean emissivity, $\bar{\varepsilon}$, and particle radius, r. This cooling time for the plume observed in field measurements can be analyzed to yield mean particle emissivity, $\bar{\varepsilon}$. This result, combined with a measure of $\varepsilon_\lambda/\bar{\varepsilon}$ as previously discussed, yields ε_λ.

The purpose of this work is to provide a basis for rocket-plume infrared data analysis. Once such measurements determine the emissivity of the rocket exhaust particles, more accurate predictions of particle plume radiant emission profiles can be made.

References

1 Radke, H. H., Delaney, L. J., and Smith, P., "Exhaust Particle Size Data from Small and Large Solid Rocket Motors," TOR-1001(S2951-18)-3, July 1967, Aerospace Corp., San Bernardino Operations Div., San Bernardino, Calif.

2 Jenkins, R. M. and Hoglund, R. F., "A Uniform Theory of Particle Growth in Rocket Chambers and Nozzles," AIAA Paper 69-541, U.S. Air Force Academy, Colo., 1969.

3 Hoglund, R. F., "Recent Advances in Gas-Particle Nozzle Flows," *ARS Journal*, Vol. 32, No. 5, May 1962, pp. 662–671.

4 Morizumi, S. J. and Carpenter, H. J., "Thermal Radiation from the Exhaust Plume of an Aluminized Composite Propellant Rocket," *Journal of Spacecraft and Rockets*, Vol. 1, No. 5, Sept.–Oct. 1964, pp. 501–507.

5 Hoffman, R. J., English, W. D., Oeding, R. G., and Weber, W. T., "Plume Contamination Effects Prediction, The Contam Code Computer Program," AFRPL-TR-71-109, Dec. 1971, Air Force Rocket Propulsion Lab., Edwards Air Force Base, Calif.

6 Cherry, S. S., Thomas, M., and Younkin, R. L., "Rocket Plume Optical Signature," CR-5-244, Oct. 1972, McDonnell Douglas Astronautics Co.—West, Huntington Beach, Calif.

7 Plass, G. N., "Mie Scattering and Absorption Cross Sections for Aluminum Oxide and Magnesium," *Applied Optics*, Vol. 3, No. 7, July 1964, pp. 867–872.

8 Bauer, E. and Carlson, D. J., "Mie Scattering Calculations for Micron Size Alumina and Magnesia Spheres," *Journal of Quantitative Spectroscopy and Radiative Transfer*, Vol. 4, No. 3, May–June 1964, pp. 363–374.

9 Stull, D. R. and Prophet, H., *JANAF Thermochemical Tables*, 2nd ed., NSRDS-NBS 37, June 1971, National Bureau of Standards, Washington, D.C.

10 Streed, E. R., Cunnington, G. R., and Liu, C. K., "TARGET PHENOMENOLOGY: Task III: Experimental Determination of the Infrared Spectral Optical Properties of Bulk and Powered Aluminum Oxide (U)," LMSC Rept. D313095, TP-3550, (AFRPL Report 73-3), Dec. 1972, Lockheed Missiles and Space Co., Palo Alto, Calif.

Effective Moduli of Layered Composites

C. H. S. Chen* and F. Tabaddor†

The B. F. Goodrich Company, Akron, Ohio

Introduction

FORMULA for obtaining the effective moduli (or stiffnesses) of laminated composites are given in many references.[1–4] However, except for Ref. 4, they are all limited only to two-dimensional quantities (3 × 3 matrix) since the majority of composites are in the form of thin plates or shells. But when the layered composites are not in the form of thin plates or shells or when the plate or shell models are not suitable for the analysis, the layered composite has to be treated as anisotropic solid. In this case the properties associated with third direction can not be neglected. Therefore, it is necessary to generate a complete 6 × 6 matrix for elastic moduli which takes into account the properties in all three directions. The objective of this Note is to derive the complete moduli matrix for the class of anisotropic solid composed of layered media. In the present Note no limitation is imposed on the type of anisotropy each constituent layer can possess, whereas in Ref. 4 it is restricted to monoclinic anisotropy. Therefore the present treatment is more general than that of Ref. 4 and that it is carried out in more concise form, although the approaches of both are in principle the same. Explicit expressions are obtained for two-layered angle ply composite which is of most common interest to us. Although only the gross or approximate properties in the sense of composite theory are obtained here, they can be used in solving three-dimensional problems.

Received June 27, 1973; revision received November 20, 1973.

Index category: Structural Composite Materials.

* Senior Engineering Scientist. Member AIAA.

† Senior Engineering Scientist.

Basic Equations

Consider an infinitesimal element of composite media made of n layers of anisotropic material (Fig. 1). Each layer may have its planes of elastic symmetry in arbitrary orientation with respect to coordinate system. For the case of fiber reinforced material this implies that each layer may have arbitrary fiber orientation with respect to coordinate axes. Let us apply to this element a constant strain field $[\bar{e}_x]$ and constant stress field $[\bar{s}_z]$ where

$$[\bar{e}_x] = \begin{bmatrix} \bar{\varepsilon}_x \\ \bar{\varepsilon}_y \\ \bar{\gamma}_{xy} \end{bmatrix}, \qquad [\bar{s}_z] = \begin{bmatrix} \sigma_z \\ \tau_{yz} \\ \tau_{xz} \end{bmatrix} \qquad (1)$$

It should be stated here that some of the notations used here may not have the same meanings as those commonly used in laminated plate theory and the readers should be cautious not to be confused with their definitions. The stress-strain relations for ith layer may then be written as

$$\begin{bmatrix} s_x^{\,i} \\ \bar{s}_z \end{bmatrix} = \begin{bmatrix} A_i & H_i \\ H_i^T & C_i \end{bmatrix} \begin{bmatrix} \bar{e}_x \\ e_z^{\,i} \end{bmatrix} \qquad (2)$$

where

$$[s_x] = \begin{bmatrix} \sigma_x \\ \sigma_y \\ \tau_{xy} \end{bmatrix}, \qquad [e_z] = \begin{bmatrix} \varepsilon_z \\ \gamma_{yz} \\ \gamma_{xz} \end{bmatrix} \qquad (3)$$

with superscript and subscript i denoting ith layer and superscript T denoting matrix transpose. A_i, H_i, C_i, and H_i^T are sub-matrices in stiffness matrix. It should be noted here that A_i and C_i are both symmetric matrices.

Equations (2) give us

$$s_x^{\,i} = A_i \bar{e}_x + H_i e_z^{\,i} \qquad (4)$$

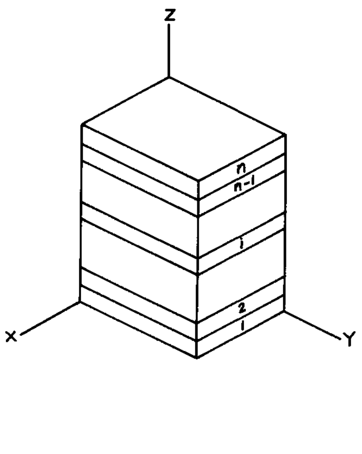

Fig. 1 Element of layered composite.

$$e_z^i = C_i^{-1}\bar{s}_z - C_i^{-1}H_i^T\bar{e}_x \tag{5}$$

where for brevity the matrix symbol [ ] has been omitted.

Without loss of generality all the layers are assumed to have the same thickness. Then the average stress s_x and the average strain ϵ_z for the element are expressed as

$$\begin{aligned} s_x &= \frac{1}{n}\Sigma s_x^i \\ &= \bar{e}_x\frac{1}{n}\Sigma A_i + \frac{1}{n}\Sigma H_i e_z^i \end{aligned} \tag{6}$$

$$\begin{aligned} e_z &= \frac{1}{n}\Sigma e_z^i \\ &= \bar{s}_z\frac{1}{n}\Sigma C_i^{-1} - \bar{e}_x\frac{1}{n}\Sigma C_i^{-1}H_i^T \end{aligned} \tag{7}$$

Substituting Eq. (5) into (6) we get

$$s_x = \bar{e}_x\frac{1}{n}\Sigma(A_i - H_i C_i^{-1}H_i^T) + \bar{s}_z\frac{1}{n}\Sigma H_i C_i^{-1} \tag{8}$$

Let $P = (1/n)\Sigma(A_i - H_i C_i^{-1}H_i^T)$, $E = (1/n)\Sigma H_i C_i^{-1}$, $F = (1/n)\Sigma C_i^{-1}$, and notice here that, since C_i is symmetric, C_i^{-1} and F are also symmetric and it can be shown that $\Sigma C_i^{-1}H_i^T = (\Sigma H_i C_i^{-1})^T = E^T$. This allows Eqs. (8) and (7) to be written as

$$s_x = P\bar{e}_x + E\bar{s}_z \tag{9}$$

$$e_z = F\bar{s}_z - E^T\bar{e}_x \tag{10}$$

From Eq. (10) we obtain

$$\bar{s}_z = F^{-1}e_z + F^{-1}E^T\bar{e}_x \tag{11}$$

Substituting Eq. (11) into Eq. (9) yields, together with Eq. (11),

$$\begin{bmatrix} s_x \\ \bar{s}_z \end{bmatrix} = \begin{bmatrix} P + EF^{-1}E^T & EF^{-1} \\ F^{-1}E^T & F^{-1} \end{bmatrix}\begin{bmatrix} \bar{e}_x \\ e_z \end{bmatrix} \tag{12}$$

Equations (12) is the average stress-strain relations of the layered media. Here, again, because F^{-1} is symmetric, hence it follows from matrix algebra that $F^{-1}E^T = (EF^{-1})^T$ and the equivalent stiffness matrix is symmetric.

Example

For the purpose of demonstration let us consider a two-ply composite ($n = 2$) of $\pm\alpha$ fiber orientation with planes of elastic symmetry parallel to x-y plane. For this unidirectional composite we have

$$A_i = \begin{bmatrix} A_{11} & A_{12} & \pm A_{16} \\ & A_{22} & \pm A_{26} \\ \text{sym.} & & A_{66} \end{bmatrix}, \quad H_i = \begin{bmatrix} A_{13} & 0 & 0 \\ A_{23} & 0 & 0 \\ \pm A_{36} & 0 & 0 \end{bmatrix},$$

$$C_i = \begin{bmatrix} A_{33} & 0 & 0 \\ & A_{44} & \pm A_{45} \\ \text{sym.} & & A_{55} \end{bmatrix} \tag{13}$$

and

$$C_i^{-1} = \begin{bmatrix} \frac{1}{A_{33}} & 0 & 0 \\ & \frac{A_{55}}{\Delta_{45}} & \pm\frac{A_{45}}{\Delta_{45}} \\ \text{sym.} & & \frac{A_{44}}{\Delta_{45}} \end{bmatrix}$$

where $\Delta_{45} = A_{44}A_{55} - A_{45}^2$ and the top sign applies to $i = 1(+\alpha)$ and the bottom sign to $i = 2(-\alpha)$.

From them we obtain

$$P = \begin{bmatrix} \beta_{11} & \beta_{12} & 0 \\ \beta_{12} & \beta_{22} & 0 \\ 0 & 0 & \beta_{66} \end{bmatrix}, \quad E = \begin{bmatrix} \frac{A_{13}}{A_{33}} & 0 & 0 \\ \frac{A_{23}}{A_{33}} & 0 & 0 \\ 0 & 0 & 0 \end{bmatrix},$$

$$F = \begin{bmatrix} \frac{1}{A_{33}} & 0 & 0 \\ 0 & \frac{A_{55}}{\Delta_{45}} & 0 \\ 0 & 0 & \frac{A_{44}}{\Delta_{45}} \end{bmatrix}$$

$$F^{-1} = \begin{bmatrix} A_{33} & 0 & 0 \\ 0 & A_{44} - \frac{A_{45}^2}{A_{55}} & 0 \\ 0 & 0 & A_{55} - \frac{A_{45}^2}{A_{44}} \end{bmatrix} \tag{14}$$

where $\beta_{ij} = A_{ij} - A_{i3}A_{j3}/A_{33}$ ($i = 1, 2, 6$). We finally obtain the effective moduli as

$$\begin{bmatrix} A_{11} & A_{12} & 0 & A_{13} & 0 & 0 \\ & A_{22} & 0 & A_{23} & 0 & 0 \\ & & A_{66} - \frac{A_{36}^2}{A_{33}} & 0 & 0 & 0 \\ & & & A_{33} & 0 & 0 \\ & \text{sym.} & & & A_{44} - \frac{A_{45}^2}{A_{55}} & 0 \\ & & & & & A_{55} - \frac{A_{45}^2}{A_{44}} \end{bmatrix} \tag{15}$$

Identical result can be obtained using Eqs. (7–9) of Ref. 4. Equation (15) shows that this two layered composite is orthotropic and the simple averaging process is applicable in obtaining the effective moduli except the shear rigidities.

It should be emphasized here that the present derivation is primarily for equivalent homogeneous properties of three-dimensional anisotropic solid. However, some remark will be made on its applications to plates and shells. Notice that, in Eq. (15), the shear rigidity in the x-y plane is now $(A_{66} - A_{36}^2/A_{33})$ instead of only A_{66} which is for classical homogeneous plate or shell type structure. This is because in the latter case, conventionally, we are only dealing with A_i in Eq. (2) and consequently the term A_{36}^2/A_{33} simply does not appear. For laminated plates or shells, if the normal stress $\bar{\sigma}_z$ is negligible, we obtain from third of Eq. (15)

$$\varepsilon_z = -\frac{1}{A_{33}}(A_{13}\bar{\varepsilon}_x + A_{23}\bar{\varepsilon}_y) \tag{16}$$

By substituting Eq. (16) into the rest of Eq. (15), we have for membrane properties

$$[s_x] = [P][\bar{e}_x] \tag{17}$$

Equation (17) can also be obtained by simple averaging of the quantities for single layer given by Whitney[5] or Ashton and Whitney.[6] Although Eq. (17) may be used in obtaining the in-plane stiffnesses of the classical laminated plate or shell, in general it is not advisable to be used in calculating the bending stiffnesses unless the composite can be considered as equivalent homogeneous, for example the layered medium with repeating layer pattern as mentioned in Ref. 4.

Similarly, for the applications of the present results of effective moduli to plates or shells of laminated type including transverse shear effect, homogeneous plate and shell theories such as developed by Ambartsumyan[1,7] should be used instead of laminated plate theory such as given in Refs. 5 and 6. The comparison of the two theories is out of the scope of this Note and will be attempted in future, but in general it may be said that as the number of repetition of the repeating layer pattern increases the accuracy of the homogeneous plate theory will be improved. However, if the number of layers is small, laminated plate theory will yield better result.

As a final remark, we again emphasize that the present result is best suited for application to anisotropic solids, plates, and shells which are considered to be homogeneous. It is also suitable for application to plates or shells when effects associated with transverse normal strain (or stress) are considered.[8] It is reported in Ref. 8 that sometimes this effect may exceed that of transverse shear.

References

[1] Ambartsumyan, S. A., *Theory of Anisotropic Shells,* NASA TT F-118, May 1964, Chap. II, p. 34.

[2] Calcote, L. R., *The Analysis of Laminated Composite Structures,* Van Nostrand Reinhold, New York, 1969, Chap. 3, p. 53.

[3] Lehnitskii, S. G., *Anisotropic Plates,* Gordon and Breach, New York, 1968, Chap. 9, p. 301.

[4] Chou, P. C. et al., "Elastic Constants of Layered Media," *Journal of Composite Materials,* Vol. 6, 1972, p. 80.

[5] Whitney, J. M., "The Effect of Transverse Shear Deformation on the Bending of Laminated Plates," *Journal of Composite Materials,* Vol. 3, 1969, p. 534.

[6] Ashton, J. E. and Whitney, J. M., *Theory of Laminated Plates,* Technomic, Stamford, Conn., 1970.

[7] Ambartsumyan, S. A., *Theory of Anisotropic Plates,* Technomic, Stamford, Conn., 1970.

[8] Ambartsumyan, S. A., "A New Refined Theory of Anisotropic Shells," *Mechanika Polimerov,* No. 5, 1970, p. 884.

Analysis and Test of a Precision Pulse-Rebalance Gyroscope

R. N. CLARK*
University of Washington, Seattle, Wash.
AND
D. C. FOSTH†
The Boeing Company, Seattle, Wash.

Introduction

THE advantages of pulse-rebalance schemes for inertial instruments, as compared to continuous rebalance techniques, are especially important where a digital computer is used to process the signals provided by these instruments.[1-7] A method for deriving the rebalance signal which uses a triangular wave modulation of the gyro signal is described here. This method is intended for use in strapdown attitude reference systems of advanced spacecraft and missiles.[3]

The purpose of the analysis and tests described here was twofold. First, a compensation network which assured a high static gain of the control loop and stability was required. Without this compensation the control loop exhibited a prominent limit cycle oscillation, which had to be eliminated by the compensation. Second, the steady-state accuracy of the entire system was to be determined to assess the suitability of this instrument for strap-down applications. Both attitude and attitude rate can be determined from the signal provided by this instrument.

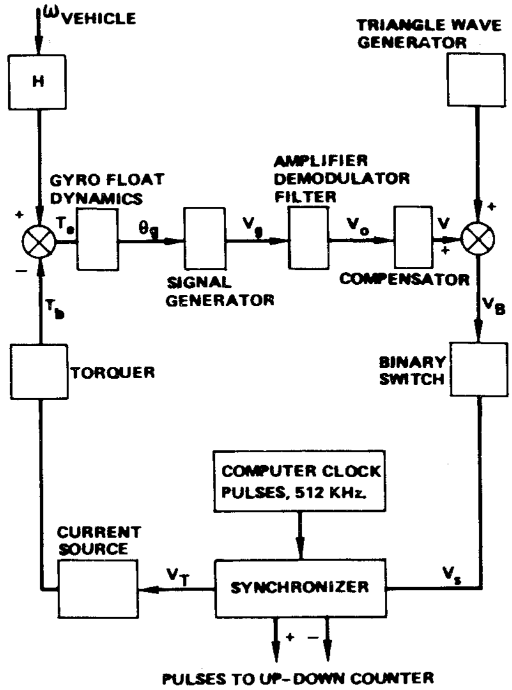

Fig. 1 Block diagram of complete system.

Discrete Pulse-Width Modulated Rebalance System

The gyroscope used here is a Honeywell model GG334A3 single degree of freedom, gas bearing rotor, floated instrument. A block diagram of the entire gyro control loop showing how the digital signal is provided appears in Fig. 1. The transfer function representing the float dynamics is

$$\theta_g(s)/T_e(s) = (1/J)/s(s+C/J)$$

where C and J have the numerical values listed in Table 1. The signal generator is excited by 8 volts (rms) at a precisely controlled frequency of 6.4 KHz, giving the sensitivity listed in Table 1. A conventional phase-sensitive demodulator (with amplification) produces a full-wave rectified signal whose average value is proportional to θ_g, the angular deflection of the output axis. The sensitivity of the amplifier-demodulator combination is 9 v (average value) per volt (rms). An active filter is used to smooth the full wave rectified output from the demodulator and to provide gain. The dynamics of this filter are chosen so that very little distortion of the (relatively) slowly fluctuating signal will occur while considerable smoothing of

Table 1 Physical characteristics of Honeywell GG334A3 gyroscope

Wheel momentum, H	2×10^5 GR(cm)^2(sec)$^{-1}$
Moment of inertia of float Assembly about output axis, J	225 GR(cm)^2
Damping coefficient of Float about output axis, C	2.5×10^5 dyne-cm-sec.
Signal generator sensitivity, (Excitation 8 v, 6.4 KHz)	18.7 mv (rms) per mrad
Torquer sensitivity	1.03×10^3 dyne-cm per ma

Received June 18, 1973; revision received November 2, 1973. The authors wish to acknowledge the contributions to the electronic design of the digital circuits and the design of the demodulator filters made by J. M. Folline and R. VanSickle. Constructive suggestions by the reviewers are also acknowledged.

Index categories: Data Sensing and Presentation or Transmission Systems; Spacecraft Attitude Dynamics and Control.

* Professor of Electrical Engineering; also Consultant, The Boeing Company, Sensors, Guidance, and Control Dept., Aerospace Group.

† Senior Specialist Engineer, Sensors, Guidance, and Control Dept., Aerospace Group.